Improving Robustness Against Variation in Resonance Frequency for Repeater of Resonant Inductive Coupling Wireless Power Transfer Systems

Masataka Ishihara, Shoma Ohata, Keita Fujiki, Kazuhiro Umetani, Eiji Hiraki
Graduate School of Natural Science and Technology
Okayama University
Okayama, Japan

Published in: 2018 20th European Conference on Power Electronics and Applications (EPE'18 ECCE Europe)

Link: https://ieeexplore.ieee.org/document/8515386

Improving Robustness Against Variation in Resonance Frequency for Repeater of Resonant Inductive Coupling Wireless Power Transfer Systems

Masataka Ishihara, Shoma Ohata, Keita Fujiki, Kazuhiro Umetani, Eiji Hiraki
OKAYAMA UNIVERSITY
3-1-1 Tsushima-naka, Kita-ku
Okayama, Japan
Tel.: +81 / (86) – 251.8115.
Fax: +81 / (86) – 251.8258.
E-Mail: p4wv0vf6@s.okayama-u.ac.jp
URL: http://www.okayama-u.ac.jp/

Keywords

«Wireless power transmission», «Contactless Energy Transfer», «Circuits»

Abstract

Intermediate resonators (repeaters) for resonant inductive coupling wireless power transfer have been widely studied as a method of improving not only the transmission distance but also the output power. For the repeater to operate effectively, it is needed to induce a large current in the repeater to enhance the magnetic field far from a transmitting resonator. However, it is often difficult to induce a large current in the repeater due to frequency splitting phenomenon. This phenomenon easily occurs when the resonator having high quality factor such as the repeater is used. The frequency characteristic of the induced current in the repeater has multiple peaks when the frequency splitting phenomenon occurs. In addition, these multiple peaks shift according to slight variation in the parameters of the coil and the capacitor that constitute the resonator. This slight variation is easily caused by production error, temperature characteristic, and aging degradation of the coil and the capacitor. The induced current in the repeater is significantly decreased by the slight variation in the parameters, namely, the slight variation in the resonance frequency. Therefore, the repeater has low robustness against variation in the resonance frequency. To address these difficulties, we apply an auxiliary circuit to the repeater. The auxiliary circuit can dynamically adjust a phase of the induced current in the repeater, namely, the resonance frequency without complicated control. As a result, a large induced current can be maintained even if the frequencies corresponding to the peaks shift. Consequently, we can provide the repeater having a stable characteristic against the variation in the resonance frequency. The effectiveness of the repeater applied the auxiliary circuit and the appropriateness of analysis results are supported with simulation and experimental results.

Introduction

Wireless power transfer (WPT) techniques are promising to realize a convenient, safe, and reliable power supply because physical cable connections can be removed. In particular, the resonant inductive coupling wireless power transfer (RIC-WPT) using magnetic coupling between coils is now under the spotlight as a high efficiency WPT technique for various applications. For low power applications such as household appliances [1], mobile devices [2], biomedical devices [3], To transfer enough power is important even if the transmission distance of the WPT increases.

However, an area where enough power can be received is quite limited because the magnitude of the magnetic coupling significantly decreases as the transmission distance increases. Especially in low power applications, this difficulty is serious because a receiving resonator (receiver) is usually small due to the limited size of installation area. The small-sized receiver tends to be difficult to collect the enough magnetic flux. As a result, the transmission distance of the low power application is usually short. Therefore, the challenge of the transmission distance needs to be overcome for the wide adoption of the RIC-WPT for the low power applications.

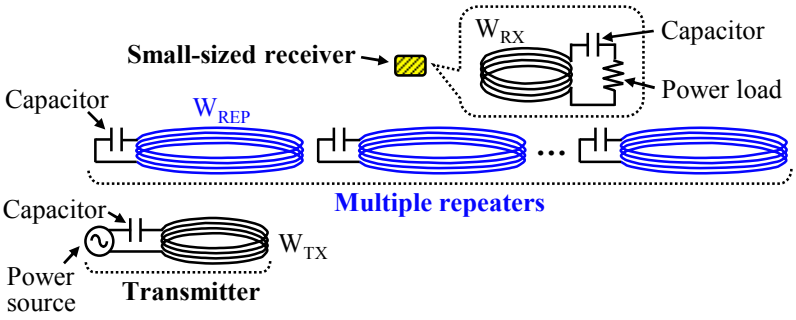

Fig. 1: RIC-WPT system with multiple repeaters for low power application.

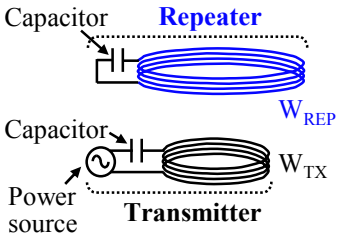

Fig. 2: Simplified analytical model for this study.

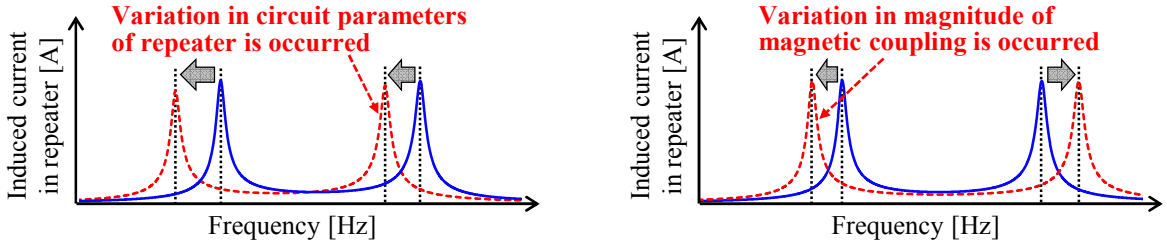

(a) Influence of variation in resonance frequency (b) Influence of variation in magnetic coupling

Fig. 3: Frequency splitting phenomenon of Figure 2.

To address this difficulty, it has been actively investigated to place the intermediate resonators (repeaters) which relay the magnetic field from the transmitting resonator (transmitter) to the receiver [1, 3–10]. As shown Fig. 1, an arbitrary number of repeaters can be utilized by adding in-between the transmitter and the receiver [7–10], where W_{TX}, W_{REP} and W_{RX} represent a transmitting, repeating, and receiving coils, respectively. The repeater has generally high quality-factor (Q-factor) about several hundreds because the repeater consists of the only passive components. Therefore, large current can be sensitively induced in the repeater by little flux generated by the transmitter or other repeaters. As a result, the repeater can enhance the magnetic field far from other resonators because the induced current in the repeater generate the magnetic field around itself. Hence, the repeater can extend the area where the receiver can receive the enough power [6].

In spite of this attractive feature, it is often difficult to induce a large current in the repeater due to frequency splitting phenomenon [9–15]. The frequency characteristic of the induced current in the repeater has usually two or more peaks due to the frequency splitting phenomenon. As the previous study pointed out [11–13], the frequency splitting phenomenon easily occurs as the Q-factor of the resonator becomes higher. Actually, it is difficult to discuss the frequency splitting phenomenon of the RIC-WPT system with the multiple repeaters. Magnetic coupling between the multiple repeaters may cause more than two peaks in the frequency characteristic of the repeater current [10]. Therefore, this paper limits the discussion to the basic cases which has only one repeater for simplicity as shown in Fig. 2. In the model of Fig. 2, there are no more than two peaks in the frequency characteristic of the repeater current. Moreover, in this model, the small-sized receiver is ignored because the small-sized receiver usually uses only little flux to receive the power. In other words, it is assumed the induced current in the repeater is not affected by the small-sized receiver. To operate the repeater effectively, one of frequency corresponding to the peaks must nearly equal to the operating frequency of the power source. However, as shown Fig. 3, the frequency corresponding to the peaks shift for the following two factors.

- Slight variation in the natural resonance frequency caused by production error, temperature characteristic, and aging degradation of the coil and the capacitor that constitute resonator (See Fig. 3 (a)).
- Variation in the magnitude of the magnetic coupling according to the relative location of the repeater (See Fig. 3 (b)) [9, 11–14].

Therefore, the robustness of the repeater current against the above two factors is low. Hence, the repeater is not practical because the repeater may only operate effectively under few specific conditions.

To improve the robustness, it must be needed to adjust dynamically the resonance frequency of the repeater according to the various conditions. As a result, it may be realized to expand stably the area where the receiver can receive the enough power by freely placing an arbitrary number of repeaters as shown in Fig. 1.

Several techniques were previously proposed to adjust dynamically the resonance frequency of a resonator [14, 16–19]. In particular, a simple auxiliary circuit named Automatic Tuning Assist Circuit (ATAC) [19] may be promising compared with other techniques because the ATAC can adjust the resonance frequency without complicated control. The ATAC is originally proposed to adjust the resonance frequency of the transmitter [19]. The ATAC can adjust the phase of current and realize the unity power factor without any controller. In the previous study [19], the effectiveness of the ATAC is successfully verified under conditions that the frequency splitting phenomenon does not occur. However, it was still unknown to the effectiveness of the ATAC when the frequency splitting phenomenon occurs.

Recently, by the previous study of our group [4], the effectiveness of the ATAC has been confirmed even when the frequency splitting phenomenon occurs. According to [4], by applying the ATAC to the repeater, it is elucidated that a relatively large current in the repeater can be maintained even if the magnitude of the magnetic coupling changes as shown in Fig. 3 (b). However, the effectiveness of the ATAC is still unknown when there is variation in the natural resonance frequency under the condition in which the frequency splitting phenomenon occurs as shown in Fig. 3 (a). In addition, mathematical analysis in [4] was limited to cases in which the circuit parameters of the transmitter and the repeater are symmetric for simplicity.

Therefore, the purpose of this paper is to improve the robustness of the performance of the repeater against the influence of the variation in the natural resonance frequency by applying the ATAC to the repeater. Moreover, to analyze the variation in the natural resonance frequency, we extend the mathematical analysis of [4] so that it can be analyzed in a system in which the transmitter and the repeater are asymmetric.

The following discussion consists of four sections. Section 2 reviews the operating principle of the ATAC, section 3 analyzes Fig. 2 to which the ATAC is applied. Section 4 presents experimental and simulation results to verify the effectiveness of the ATAC and the appropriateness of the theoretical analysis results. Finally, section 5 presents the conclusions.

Operating Principle of ATAC

Firstly, we review that how the ATAC adjusts the phase of the current in the resonator by using Fig. 4. Fig. 4 consists of the voltage source V_s, the coil L, the capacitor C, the parasitic resistor r, and the ATAC. The ATAC is formed as a full-bridge circuit. The DC bus line of the ATAC has only the smoothing capacitor C_A which has the capacitance sufficiently larger than the capacitor C.

As shown in Fig. 5, the switches Q_1–Q_4 constituting the ATAC operate at the same frequency as V_s. Besides, the Q_1–Q_4 operate with the constant phase difference φ with respect to V_s. Therefore, the ATAC equivalently works as the AC voltage source as shown in Fig. 6, where V_A is the effective value of the fundamental wave component of the rectangular wave voltage generated by the ATAC.

As shown in Fig. 7, the current I_L in the resonator is decided by the superposition of the current I_s generated by V_s and the current I_A generated by $-V_A$. V_s and V_A are connected in opposite directions.

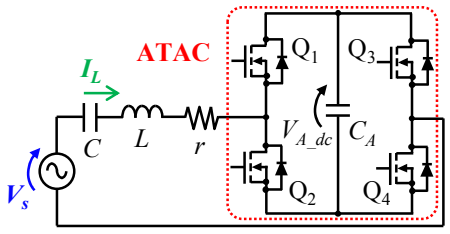

Fig. 4: Single resonator with ATAC.

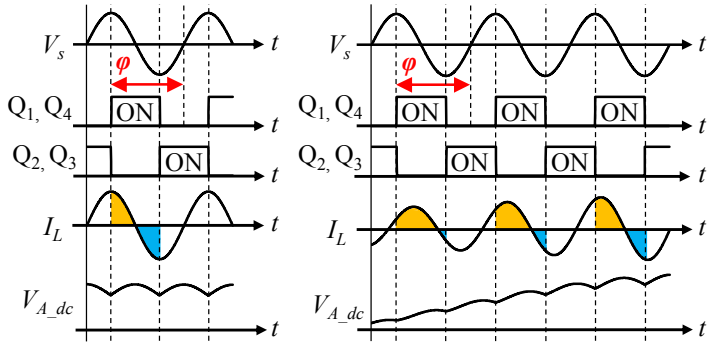

(a) Steady state (b) Transient state

Fig. 5: Schematic waveforms ATAC.

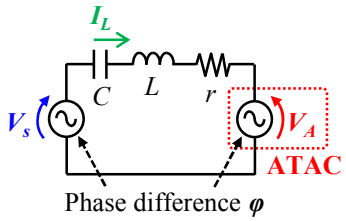

Fig. 6: Equivalent circuit of Fig 4.

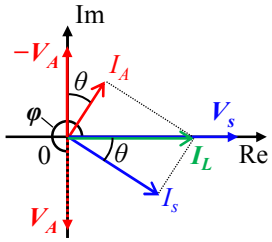

Fig. 7: Phasor diagram of Fig 6 in steady state.

Therefore, the sign of V_A is reversed. I_s is the current when the ATAC is not applied to the resonator; the phase θ of I_s is uniquely decided by the impedance of the resonator and the frequency of V_s. Therefore, the phase of the current in the resonator I_L can be changed by adding the ATAC.

The ATAC does not have ideally a resistive component as shown in Fig. 4. Therefore, in the steady state as shown in Fig. 5 (a), the time integrations of the current for charging and discharging the C_A must be equal with each other. In other words, in steady state, the phase difference between V_A and I_L is always $\pm\pi/2$. Hence, the ATAC can adjust the phase of I_L by only setting phase difference φ between V_A and V_s without complicated control.

However, as the previous study [4, 19] pointed out, a set range of φ that can be used is limited. To generate a DC voltage in C_A, in the initial operation, the time integrations of the current for charging the C_A must be larger than the time integrations of discharging, as shown in Fig. 5 (b). Therefore, in the circuit of Fig. 4, we must set φ to the range of $3\pi/2\leq\varphi\leq2\pi$ ($-\pi/2\leq\varphi\leq0$) when the resonator is inductive. On the other hand, we must set φ to the range of $0\leq\varphi\leq\pi/2$ when the resonator is capacitive.

In addition, as the previous study [4, 19] pointed out, the switches of the ATAC can achieve the ZVS (Zero Voltage Switching) turn-on when the phase of I_L is delayed by $\pi/2$ with respect to $-V_A$ in the steady state. However, attention should be given to the fact that the switches of the ATAC operate under HS (Hard Switching) turn-on when the phase of I_L is advanced by $\pi/2$ with respect to $-V_A$ in the steady state.

Theoretical Analysis of Repeater with ATAC

The purpose of this section is to formulate characteristics of the repeater to which ATAC is applied. Moreover, to improve the robustness of the repeater current, we will indicate that how to decide the phase difference of the ATAC.

In order to achieve these purposes, we firstly analyze the current in each resonator to which the ATAC is not applied by using the equivalent circuit as shown in Fig. 8. This figure shows the equivalent circuit of Fig. 2. Symbol V_i is the voltage of the power source; L_{TX} and L_{REP} are the self-inductance of $\mathrm{W_{TX}}$ and $\mathrm{W_{REP}}$, respectively; M is the mutual inductance between $\mathrm{W_{TX}}$ and $\mathrm{W_{REP}}$; r_{TX} and r_{REP} are the parasitic resistance of the transmitter and the repeater, respectively; C_{TX} and C_{REP} are the capacitance. As shown Fig. 8, the transmitter and the repeater are asymmetric unlike the previous study [4].

According to Kirchhoff's voltage law, the equivalent circuit of Fig. 8 can be expressed as

$$\begin{cases} V_i = r_{\mathrm{TX}} I_\alpha + j(\omega L_{\mathrm{TX}} - 1/\omega C_{\mathrm{TX}}) I_\alpha - j\omega M I_\beta, \\ -j\omega L_{\mathrm{REP}} I_\beta + j\omega M I_\alpha = r_{\mathrm{REP}} I_\beta - j I_\beta / \omega C_{\mathrm{REP}}. \end{cases} \tag{1}$$

Then, we define the reactance as.

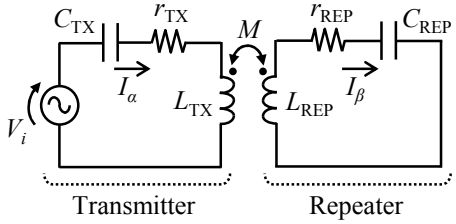

Fig. 8: Equivalent circuit of Fig 2.

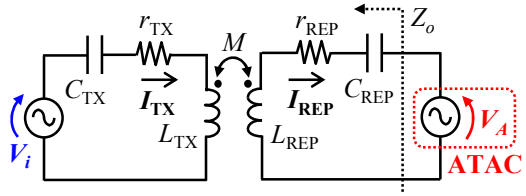

Fig. 9: Equivalent circuit of Fig 2 with ATAC.

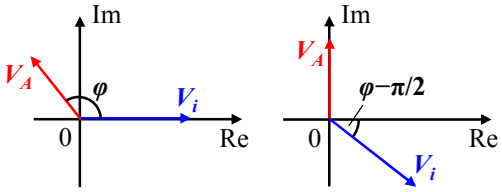

(a) Before rotation (b) After rotation

Fig. 10: Phasor diagram of Fig 9.

$$j(\omega L_{TX} - 1/\omega C_{TX}) = jX_{TX}, \quad j(\omega L_{REP} - 1/\omega C_{REP}) = jX_{REP}. \tag{2}$$

By substituting (2) into (1), the currents in the transmitter I_α and the current in the repeater I_β can be derived accordingly as

$$I_\alpha = V_i(N_{TX\text{-}R} + jN_{TX\text{-}I})/D_p, \quad I_\beta = V_i(N_{REP\text{-}R} + jN_{REP\text{-}I})/D_p, \tag{3}$$

where, $N_{TX\text{-}R}$, $N_{TX\text{-}I}$, $N_{REP\text{-}R}$, $N_{REP\text{-}I}$, and D_p are defined as

$$\begin{aligned} &N_{TX\text{-}R} = \omega^2 M^2 r_{REP} + r_{TX}\left(r_{REP}^2 + X_{REP}^2\right), \quad N_{TX\text{-}I} = \omega^2 M^2 X_{REP} - X_{TX}\left(r_{REP}^2 + X_{REP}^2\right), \\ &N_{REP\text{-}R} = \omega M(X_{TX} r_{REP} + X_{REP} r_{TX}), \quad N_{REP\text{-}I} = \omega M\left(\omega^2 M^2 + r_{TX} r_{REP} - X_{TX} X_{REP}\right), \\ &D_p = 2\omega^2 M^2\left\{r_{TX} r_{REP} - X_{TX} X_{REP} + \omega^2 M^2/2\right\} + \left(r_{TX}^2 + X_{TX}^2\right)\left(r_{REP}^2 + X_{REP}^2\right). \end{aligned} \tag{4}$$

Then, we analyze the system shown in Fig. 9 in which the ATAC is applied to the repeater. To derive the current in each resonator (I_{TX} and I_{REP}), we firstly derive the voltage of the ATAC (V_A) in the steady state. We define the phase difference φ between V_A and V_i as shown in Fig. 10 (a).

For simplicity of the analysis, we rotate the phasors of Fig. 10 (a) clockwise by $\varphi - \pi/2$. As a result, the phasor of V_A is fixed to the imaginary axis as shown in Fig. 10 (b). Then, we define I'_α and I'_β as the current in each resonator in the phasor diagram of Fig. 10 (b). Based on (3), I'_α and I'_β can be expressed as

$$\begin{aligned} &\mathrm{Re}[I'_\alpha] = V_i(N_{TX\text{-}R}\sin\varphi + N_{TX\text{-}I}\cos\varphi)/D_p, \quad \mathrm{Im}[I'_\alpha] = V_i(-N_{TX\text{-}R}\cos\varphi + N_{TX\text{-}I}\sin\varphi)/D_p, \\ &\mathrm{Re}[I'_\beta] = V_i(N_{REP\text{-}R}\sin\varphi + N_{REP\text{-}I}\cos\varphi)/D_p, \quad \mathrm{Im}[I'_\beta] = V_i(-N_{REP\text{-}R}\cos\varphi + N_{REP\text{-}I}\sin\varphi)/D_p. \end{aligned} \tag{5}$$

According to the operating principle of the ATAC, in the steady state, the phasor of I_{REP} must be orthogonal to the phasor of V_A. Therefore, $\mathrm{Im}[I_{REP}]$ is zero in the phasor diagram of Fig. 10 (b). In other words, the imaginary components of the currents generated by V_A and V_i cancel each other, i.e.

$$\mathrm{Im}[I_{REP}] = \mathrm{Im}[I'_\beta] + \mathrm{Im}[-jV_A/Z_o] = 0, \tag{6}$$

where Z_o expressed as

$$Z_o = \omega^2 M^2 r_{TX}/\left(r_{TX}^2 + X_{TX}^2\right) + r_{REP} + j\left\{X_{REP} - \omega^2 M^2 X_{TX}/\left(r_{TX}^2 + X_{TX}^2\right)\right\}. \tag{7}$$

By substituting (7) into (6), V_A can be derived as

$$V_A = V_i(-N_{REP\text{-}R}\cos\varphi + N_{REP\text{-}I}\sin\varphi)/\left\{\omega^2 M^2 r_{TX} + r_{REP}\left(r_{TX}^2 + X_{TX}^2\right)\right\}. \tag{8}$$

Then, we formulate I_{REP} by using the above analysis. I_{REP} has only real component when V_A is fixed to the imaginary axis. Moreover, I_{REP} is represented by the superposition of the current generated by V_i and V_A. Therefore, I_{REP} can be expressed as

$$\begin{aligned} I_{REP} &= \mathrm{Re}[I'_\beta] + \mathrm{Re}[-jV_A/Z_o] \\ &= V_i(N_{REP\text{-}R}\sin\varphi + N_{REP\text{-}I}\cos\varphi)/D_p + V_A\left\{\omega^2 M^2 X_{TX} - X_{REP}\left(r_{TX}^2 + X_{TX}^2\right)\right\}/D_p. \end{aligned} \tag{9}$$

Finally, we formulate I_{TX}. Similar to I_{REP}, I_{TX} is expressed as the superposition of the current generated by V_i and V_A. The current generated by V_i has already derived as shown in (5). The current generated by V_i can be easily derived by using Kirchhoff's voltage law as similar to (5). As a result, I_{TX} can be expressed as

$$I_{TX}=\sqrt{\left(\mathrm{Re}[I'_{\alpha}]+N_{REP\text{-}I}V_A/D_p\right)^2+\left(\mathrm{Im}[I'_{\alpha}]-N_{REP\text{-}R}V_A/D_p\right)^2}. \quad (10)$$

Next, we discuss that how to decide phase difference φ. To improve the robustness of the current in the repeater, the ATAC should operate so that the repeater can operate equivalently at the frequency corresponding to the peaks regardless of the operating frequency. According to the previous study [4] which assumes the parameters of the transmitter and the repeater is symmetric, Im[I_{REP}] is approximately zero at the frequencies in which I_{REP} peaks. Therefore, in the previous study, the phase of difference φ between V_i and V_A is set to $\pm\pi/2$ in order to zero for Im[I_{REP}] regardless of the operating frequency.

Actually, even if the transmitter and the repeater is asymmetric, Im[I_{REP}] is approximately zero at the frequencies corresponding to the peaks. When the approximation that $Q_{TX}Q_{REP}>>1$ is satisfied, Im[I_{REP}] is zero at the frequencies corresponding to the peaks which pointed out in the previous study [15], where Q_{TX} and Q_{REP} are the quality factor of the transmitter and the repeater, respectively. Therefore, the phase of difference φ between V_i and V_A should be set to $\pm\pi/2$ even if the transmitter and the repeater is asymmetric. As pointed out in the previous section, to generate the DC voltage in the smoothing capacitor of the ATAC, we must select an appropriate φ either $+\pi/2$ or $-\pi/2$.

Experimental and Simulation Results and Discussion

In this section, we confirm by experiment and simulation that the ATAC is effective for improving the robustness of the repeater current against the variation in the resonance frequency. In addition, we confirm the appropriateness of the analysis results of the previous section.

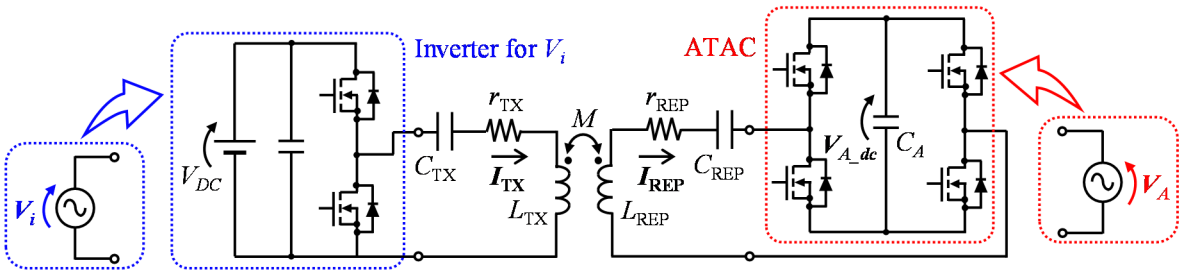

Fig. 11: Circuit configuration for experiment and simulation (w/ ATAC).

Table I: Circuit parameters

Input DC voltage	V_{DC}	4.0 V
Self-inductance of W_{TX}	L_{TX}	55.13 μH
Parasitic resistance of transmitter	r_{TX}	0.109 Ω
Capacitance of transmitter	C_{TX}	40.81 nF
Self-inductance of W_{REP}	L_{REP}	141.53 μH
Parasitic resistance of repeater	r_{REP}	0.206 Ω
Capacitance of repeater	C_{REP}	16.14 nF
Mutual inductance	M	5.41 μH
Capacitance of ATAC	C_A	22 μF (V_{A_dc} = 0 V)
Phase difference	φ	$-\pi/2$ or $+\pi/2$

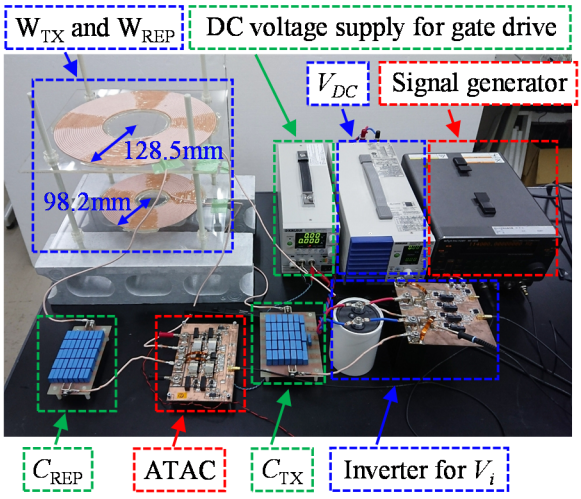

Fig. 12: Experimental setup (w/ ATAC).

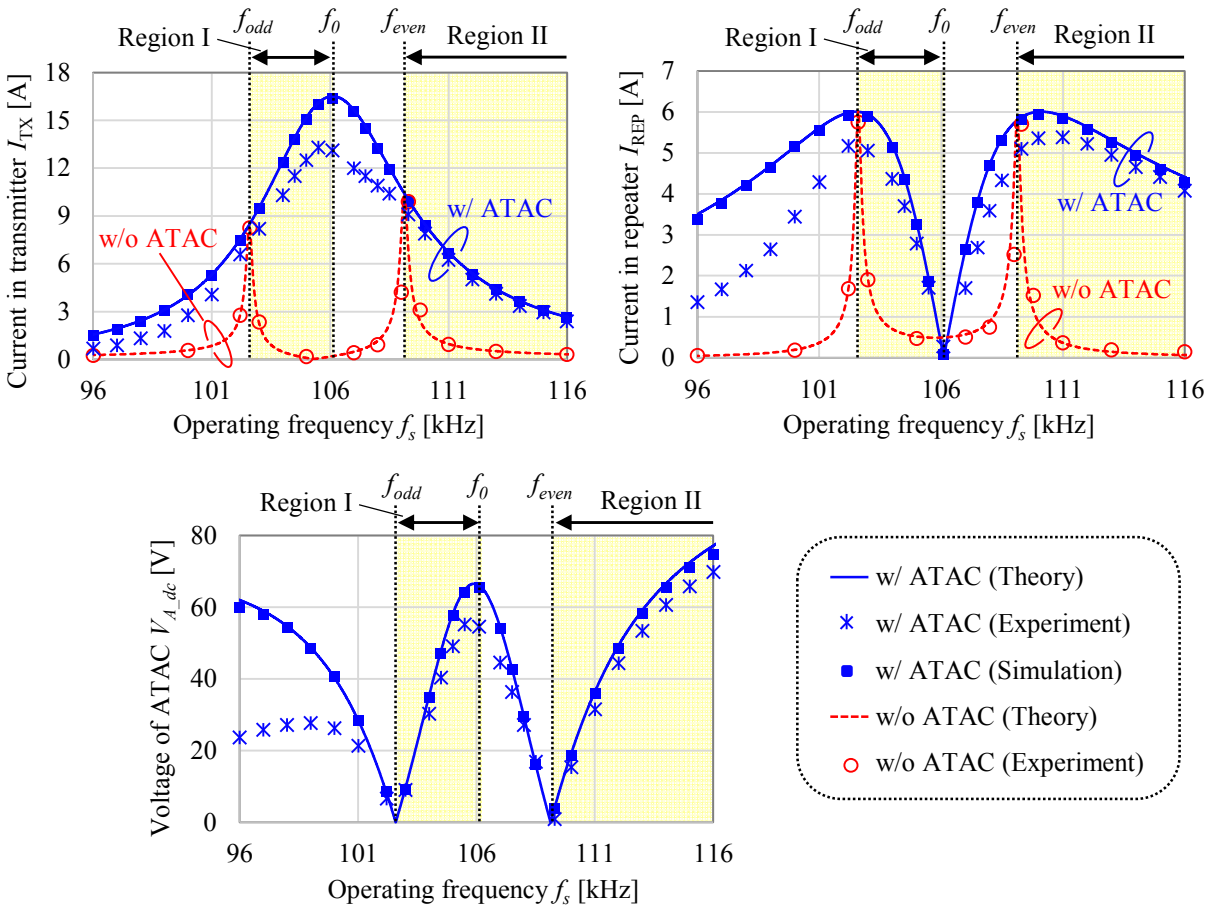

Fig. 13: Frequency characteristic of I_{TX}, I_{REP}, and V_{A_dc}.

Fig. 11 shows the circuit configuration for the experiment and the simulation. Moreover, Table I shows the circuit parameters for the experiment and the simulation. In the circuit parameters of Table I, the resonance frequencies of the transmitter and the repeater are well tuned and almost equal to each other. Fig. 12 shows the photograph of the experimental setup for the evaluation of the repeater with the ATAC. To drive the ATAC, it is necessary to self-generate the power and the control signal for driving the switches constituting the ATAC because the repeater is not connected a power source. However, in this paper, the ATAC is driven by using the external power supply and the signal generator as shown in Fig. 12. The ATAC which can independently drive will be realized by future work.

Firstly, we evaluate the frequency characteristics of I_{TX}, I_{REP}, and V_{A_dc}. The operating frequency is set from 96 kHz to116 kHz. Fig. 13 shows the experimental, simulation, and theoretical analysis results of the frequency characteristics of I_{TX}, I_{REP}, and V_{A_dc}, where f_{odd} and f_{even} are the frequencies at which I_{REP} of "w/o ATAC" reaches the peak, and f_0 is the frequency of the trough between f_{odd} and f_{even}. The phase difference φ must be set to $-\pi/2$ when the operating frequency f_s is $f_s \leq f_{odd}$ or $f_s \geq f_{even}$. On the other hand, the phase difference φ must be set to $+\pi/2$ when the operating frequency f_s is $f_{odd} < f_s < f_{even}$.

As can be seen from Fig. 13, when the ATAC is not applied to the repeater, the experimental results are corresponded well to the theoretical analysis results. In contrast, when the ATAC is applied to the repeater, the experimental results have some error with respect to the theoretical analysis results. The error is caused because the slight switching and conduction losses of the ATAC easily affect the characteristics of the resonator having high Q-factor. In fact, the simulation results without the losses of the ATAC are corresponded well to the theoretical analysis results. The switches constituting the ATAC can achieve the ZVS turn-on at the region I and the region II shown in Fig. 13. By contrast, at the regions other than the region I and the region II, the switches cannot avoid the HS turn-on. As a result, the error tends to be large at the regions excluding the region I and the region II. Therefore, it is preferable to use the ATAC at the region I or the region II. However, in practice, the region II may be better than the region I for the following three reasons. First, the region I requires a larger I_{TX} than the region II to induce the same magnitude of I_{REP}. Second, I_{REP} of region I is more susceptible to the change of the

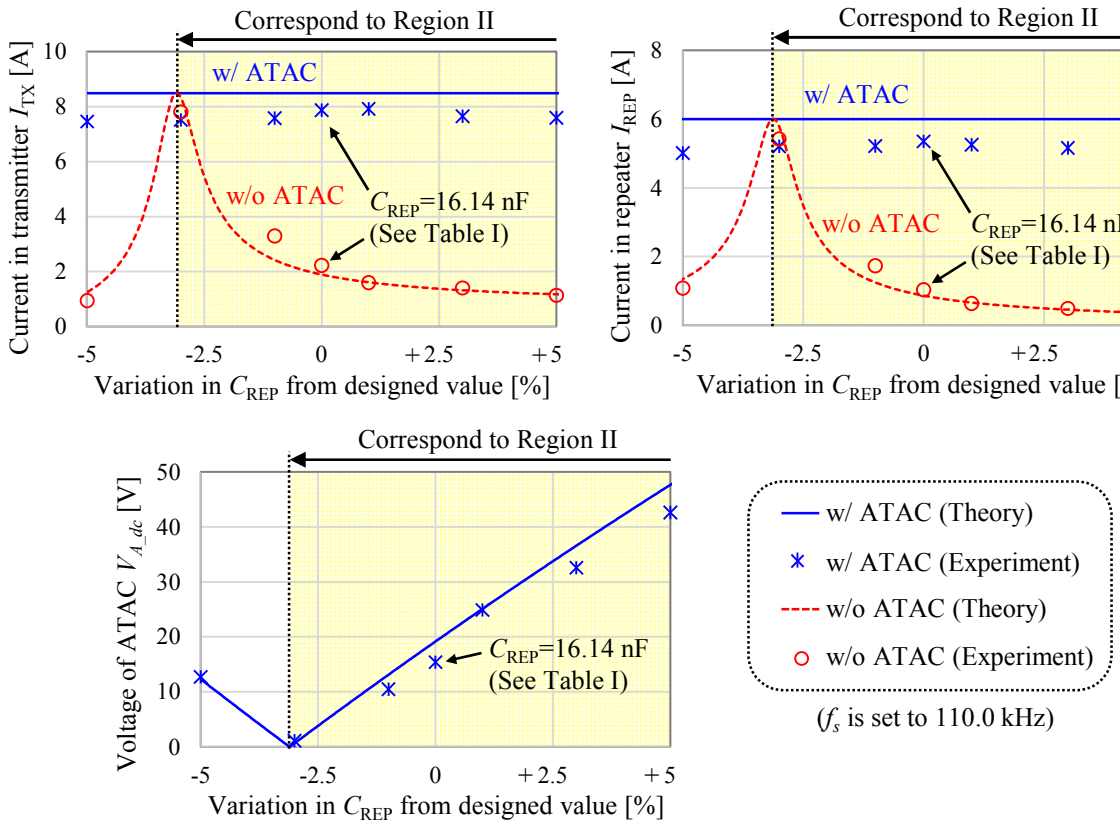

Fig. 14: Characteristic of I_{TX}, I_{REP}, and V_{A_dc} against variation in resonance frequency of repeater

operating frequency than I_{REP} of region II. Third, the region I disappears when the relation of $kQ_{TX}Q_{REP}>0$ is not satisfied [11–14], where k is coupling coefficient ($k^2=M^2/L_{TX}L_{REP}$).

Two narrow peaks appear in the frequency characteristic of I_{REP} due to the frequency splitting phenomenon when the ATAC is not applied to the repeater. The frequency characteristic with the narrow peaks cause the low robustness of I_{REP} as mentioned in the introduction. On the other hand, when the ATAC is applied to the repeater, two wide peaks appear in the frequency characteristic of I_{REP}. The frequency characteristic with the wide peaks may be able to maintain a relatively large I_{REP} even if f_{odd} and f_{even} are shifted due to the variation in the natural resonance frequency. In fact, according to the previous study [4], it is elucidated that the frequency characteristic with the wide peaks is effective for improving the robustness of I_{REP} against the variation in the magnitude of the magnetic coupling.

Then, we confirm the effectiveness of the ATAC when the natural resonance frequency of the repeater deviates from the designed value. The operating frequency f_s is set to 110.0 kHz. We evaluate the I_{TX}, I_{REP}, and V_{A_dc} when the value of C_{REP} is shifted from the designed value of table I within the range of −5 % to + 5 %. Fig. 14 shows the experimental and the theoretical analysis results. When the ATAC is not applied to the repeater, the magnitude of I_{REP} is easily fluctuated according to the variation in C_{REP}. Therefore, we cannot ignore the variation in the natural resonance frequency. On the other hand, when the ATAC is applied to the repeater, the almost constant I_{REP} can be induced in the repeater regardless of the variation in C_{REP}. Even if C_{REP} is deviated, V_{A_dc} automatically increases, and the resonance frequency of the repeater can be adjusted. Therefore, it is elucidated that ATAC is effective for improving the robustness against the variation in the natural resonance frequency of the resonator.

Conclusion

The repeater having high Q-factor of the RIC-WPT is promising to improve the transmission distance and the output power. However, the repeater has high sensitivity to the deviation in the inductance and the capacitance constituting the resonator. Therefore, the repeater has the low robustness against the variation in the natural resonance frequency. In order to approach this problem, we applied the ATAC to the repeater. As a result, it was found that the narrow peaks which appeared in the frequency characteristic of the repeater current (I_{REP}) can be widen. The frequency characteristic of I_{REP}

with the wide peaks may be able to eliminate accurately adjustment of the resonance frequency. In fact, when the ATAC is applied to the repeater, the almost constant I_{REP} can be induced in the repeater regardless of the variation in the resonance frequency. Therefore, the ATAC can improve the robustness against the variation in the natural resonance frequency even if the frequency splitting phenomenon occurs.

References

[1] Kim J., Son H.-C., Kim D.-H, Park Y. J.: Optimal design of a wireless power transfer system with multiple self-resonators for an LED TV, IEEE Trans. Consum. Electron., vol. 58, no. 3, pp. 775–780

[2] Jeong N. S., Carobolante F.: Wireless charging of a metal-body device, IEEE Trans. Microw. Theory Techn., vol. 65, no. 4, pp. 1077–1086

[3] Mirbozorgi S. A., Jia Y., Canales D., Ghovanloo M.: A wirelessly-powered homecage with segmented copper foils and closed-loop power control, IEEE Trans. Biomed. Circuits Syst., vol. 10, no. 5, pp. 979–989

[4] Ishihara M., Umetani K., Hiraki E.: Automatic resonance frequency tuning method for repeater in resonant inductive coupling wireless power transfer systems, 2018 Int. Power Electron. Conf. (IPEC-Niigata 2018 - ECCE ASIA), pp. 1610–1616

[5] Lee K., Chae S. H.: Power transfer efficiency analysis of intermediate-resonator for wireless power transfer, IEEE Trans. Power Electron., vol. 33, no. 3, pp. 2484–2493

[6] Mao S., Zhang J., Song K., Wei G., Zhu C.: Wireless power transfer using a field-enhancing coil and a small-sized receiver with low coupling coefficient, IET power electron., vol. 9, no. 7, pp. 1546–1552

[7] Lee C. K., Zhong W. X., Hui S. Y. R.: Effects of magnetic coupling of nonadjacent resonators on wireless power domino-resonator systems, IEEE Trans. Power Electron., vol. 27, no. 4, pp. 1905–1916

[8] Liu X., Wang G.: A novel wireless power transfer system with double intermediate resonant coils, IEEE Trans. Ind. Electron., vol. 63, no. 4, pp. 2174–2180

[9] Ahn D., Hong S.: A study on magnetic field repeater in wireless power transfer, IEEE Trans. Ind. Electron., vol. 60, no. 1, pp. 360–371

[10] Karaca O., Kappeler F., Waldau D., Kannel R. M., Rackles J.: Eigenmode analysis of a multiresonant wireless energy transfer system, IEEE Trans. Ind. Electron., vol. 61, no. 8, pp. 4134–4141

[11] Huang R., Zhang B., Qiu D., Zhang Y.: Frequency splitting phenomena of magnetic resonant coupling wireless power transfer, IEEE Trans. Magn., vol. 50, no. 11, 8600204

[12] Niu W.-Q., Chu J.-X., Gu W., Shen A.-D.: Exact analysis of frequency splitting phenomena of contactless power transfer systems, IEEE Trans. Circuits Syst. I, Reg. Papers, vol. 60, no. 6, pp. 1670–1677

[13] Seo D.-W., Lee J.-H, Lee H.-S.: Optimal coupling to achieve maximum output power in a WPT system, IEEE Trans. Power Electron., vol. 31, no. 6, pp. 3994–3998

[14] Trigui A., Hached S., Mounaim F., Ammari A. C., Sawan M.: Inductive power transfer system with self-calibrated primary resonant frequency, IEEE Trans. Power Electron., vol. 30, no. 11, pp. 6078–6087

[15] Zhang W., Wong S.-C., Tse C. K., Chen Q.: Analysis and comparison of secondary series- and parallel-compensated inductive power transfer systems operating for optimal efficiency and load-independent voltage-transfer ratio, IEEE Trans. Power Electron., vol. 29, no. 6, pp. 2979–2990

[16] Mai R., Liu Y., Li Y., Yue P., Cao G., He Z.: An active-rectifier-based maximum efficiency tracking method using an additional measurement coil for wireless power transfer, IEEE Trans. Power Electron., vol. 33, no. 1, pp. 716–728

[17] Osawa J., Isobe T., Tadano H.: Efficiency improvement of high frequency inverter for wireless power transfer system using a series reactive power compensator, 2017 IEEE 12th Int. Conf. on Power Electron. and Drive Syst. (PEDS), pp. 992–998

[18] Lim Y., Tang H., Lim S., Park J.: An adaptive impedance-matching network based on a novel capacitor matrix for wireless power transfer, IEEE Trans. Power Electron., vol. 29, no. 8, pp. 4403–4413

[19] Endo Y., Furukawa Y.: Proposal for a new resonance adjustment method in magnetically coupled resonance type wireless power transmission, 2012 IEEE MTT-S Int. Microw. Workshop Series on Innovative Wireless Power Transmission: Tech., Syst., and Appl. (IMWS-IWPT), pp. 263–266